IOP Publishing European Journal of Physics
Eur. J. Phys. **41** (2020) 035002 (12pp) https://doi.org/10.1088/1361-6404/ab5d93

Collision of two balls in a groove: an interplay between translation and rotation

S Gröber and J Sniatecki

Department of Physics, Technische Universität Kaiserslautern, Erwin-Schroedinger-Straße, D-67663 Kaiserslautern, Germany

E-mail: groeber@rhrk.uni-kl.de

Received 28 September 2019, revised 6 November 2019
Accepted for publication 29 November 2019
Published 24 February 2020

Abstract

When two identical balls collide with equal inital speed on a horizontal groove, one can observe three trajectory types depending on the groove width. To explain this observation, we derive velocity diagrams of the balls' motions from Newton's laws of translation and rotation and kinematics of rigid bodies in a three-dimensional vectorial representation and compare them with experimental results. The velocity diagrams and an introduced determinant allow one to discriminate between the trajectory types and to understand the interplay between translation and rotation after the collision of the balls.

Keywords: collision, video analysis, dynamics of rigid bodies

(Some figures may appear in colour only in the online journal)

1. Introduction

The motion of a single ball as well as the collision of balls influenced by impulsive, frictional or gravitational forces on flat or inclined surfaces have been extensively analysed. Studies can be roughly categorized by their theoretical treatment of ball motions mainly by treatments with conservation principles (e.g. [1, 2]) or Newton's laws of translation and rotation (e.g. [3, 4]), or a mixture of these principles and laws (e.g. [5]).

Keeping this in mind, we pick up an artificial laboratory phenomenon from [6], which can be performed with simple equipment as a qualitative freehand as well as a quantitative experiment (figure 1). Two identical balls of uniform mass distribution, radius R and mass m are released from the same height on both inclined parts of a groove. The groove width $b \in (0, 2R)$ is adjustable. One can observe three trajectory types after the first impact of the balls on the horizontal part of the groove (figure 2):

- if $b \in (0, b^*)$ is below a critical groove width b^*, the balls move away from each other;

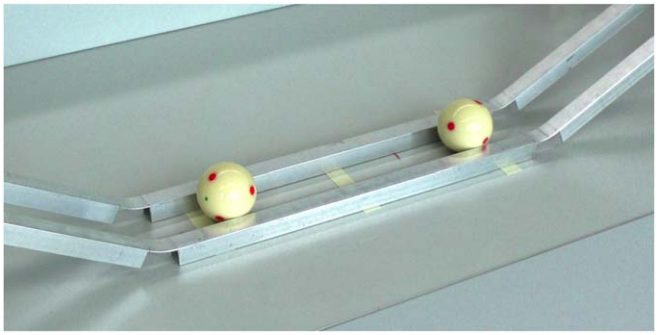

Figure 1. Setting of the experiment. Two inclined groove parts of the same inclination are used to generate equal initial ball speeds.

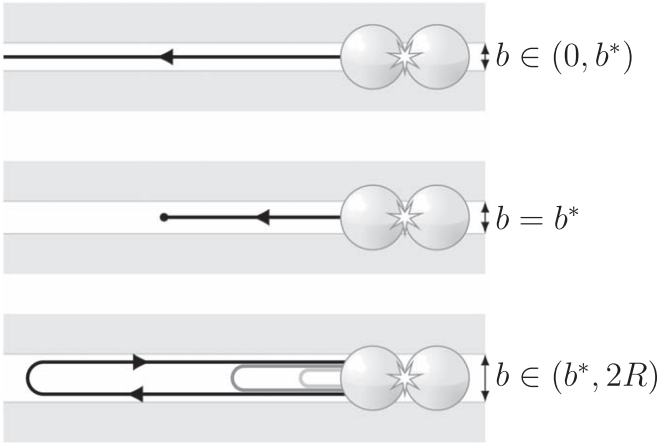

Figure 2. Trajectory types of the left ball (radius R) after the first impact for different groove widths b in respect to the critical groove width b^*.

- for $b = b^*$, the balls come to rest at a certain distance from each other; and
- if $b \in (b^*, 2R)$ is above the critical groove width b^*, the balls move away from each other, then move towards each other and collide again. This motion can appear several times with decreasing maximal distances of the balls.

The observation of these trajectory types is surprising in comparison with the seemingly similar experiment of carts colliding purely translationally on an air track. This raises the question why the balls move in such a manner. The answer requires an understanding of the connection between causes (forces and torques) and effects (translational and rotational acceleration). Therefore, we perform here a theoretical treatment of the experiment with Newton's laws of translation and rotation and not with conservation principles [6], which consider only initial and final states.

2. Derivation of the balls motion

2.1. Assumptions, particle velocities and motion states

In the following, we assume that the rolling and air friction forces acting on the balls are negligible and that the balls' collision is short, central and ideal-elastic. Moreover, we neglect

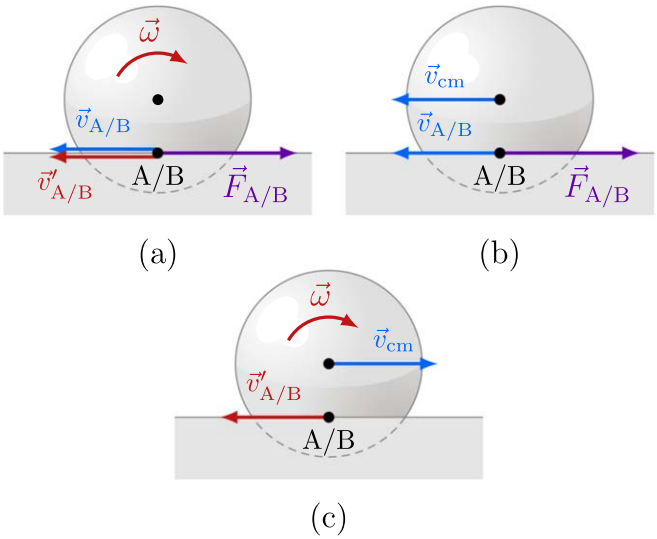

Figure 3. Motion states of (a) pure rotation, (b) pure translation and (c) pure rolling of a ball in a groove with center-of-mass velocity $\vec{v}_{\mathrm{cm}}$, velocity $\vec{v}_{\mathrm{A/B}}$ of particles in A/B with respect to an inertial reference frame, velocity $\vec{v}_{\mathrm{r}}$A/B with respect to the center of mass, angular velocity $\vec{\omega}$ and kinetic friction forces $\vec{F}_{\mathrm{A/B}}$.

tangential sliding forces between the balls during the impact. Before the first impact, the balls perform pure rolling, i.e. rolling without slipping, with the same center-of-mass speed.

Generally, the velocity $\vec{v}_{\mathrm{P}}$ of a particle in a point P of a ball in an inertial reference frame is

$$\vec{v}_{\mathrm{P}} = \vec{v}_{\mathrm{cm}} + \vec{v}'_{\mathrm{P}} = \vec{v}_{\mathrm{cm}} + \vec{\omega} \times (\vec{r}_{\mathrm{P}} - \vec{r}_{\mathrm{cm}}), \tag{1}$$

where $\vec{v}_{\mathrm{cm}}$ denotes the center-of-mass velocity in the inertial reference frame, $\vec{v}'_{\mathrm{P}}$ the velocity of the particle P relative to the center of mass, $\vec{\omega}$ the angular velocity and $\vec{r}_{\mathrm{P}} - \vec{r}_{\mathrm{cm}}$ the connecting vector from the center of mass to P.

In particular, the particles in A and B, which are currently in contact with the groove and which have the identical velocity

$$\vec{v}_{\mathrm{A/B}} = \vec{v}_{\mathrm{cm}} + \vec{v}'_{\mathrm{A/B}} = \vec{v}_{\mathrm{cm}} + \vec{\omega} \times (\vec{r}_{\mathrm{A/B}} - \vec{r}_{\mathrm{cm}}), \tag{2}$$

allow one to categorize the balls' motion states (figure 3): if one of the three velocities in (2) is zero, the magnitudes of the other two velocities are equal and we get the motion states of pure rotation ($\vec{v}_{\mathrm{cm}} = 0$, rotation without translation), pure translation ($\vec{\omega} = 0$, translation without rotation) and pure rolling ($\vec{v}_{\mathrm{A/B}} = 0$, translation and rotation without slipping) [7]. In all other cases we get intermediate motion states of translation and rotation. If the ball does not perform pure rolling, i.e. the particles in A and B move relative to the groove ($\vec{v}_{\mathrm{A/B}} \neq \vec{0}$), equal kinetic friction forces $\vec{F}_{\mathrm{A/B}}$ act on the balls in the opposite direction to the velocity $\vec{v}_{\mathrm{A/B}}$.

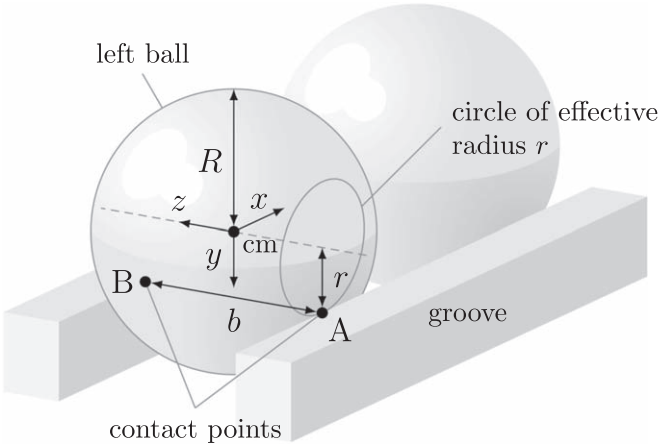

Figure 4. Fixed coordinate system and groove width b, radius R and effective radius r.

Specifically, for the fixed coordinate system in figure 4, the connecting vectors are

$$\vec{r}_{\mathrm{A/B}} = r\vec{e}_y \mp \tfrac{b}{2}\vec{e}_z \tag{3}$$

(minus for A and plus for B). Inserting (3) in (2) yields

$$\vec{v}_{\mathrm{A/B}} = v_{\mathrm{cm},x} + (\omega_z\vec{e}_z) \times (r\vec{e}_y \mp \tfrac{b}{2}\vec{e}_z) = (v_{\mathrm{cm},x} - \omega_z r)\vec{e}_x. \tag{4}$$

In (4), the tangential velocity $v_\mathrm{t} = \omega_z r$ of the particles A and B on the circle of effective radius r can be positive or negative, depending on the sign of ω_z and the direction of rotation, respectively.

In the following, due to symmetry, we consider only the motion of the left ball. The origin of the coordinate system is at the position of the center of mass of the left ball at a time $t_0 = 0$, when the balls collide (figure 4). Before the first impact ($t < t_0$) the ball performs pure rolling with center-of-mass velocity $v_{\mathrm{cm},x} > 0$ and angular velocity $\omega_z > 0$, i.e. $\vec{v}_{\mathrm{A/B}} = 0$ and from (4) follows the rolling condition

$$v_{\mathrm{cm},x} = v_\mathrm{t}. \tag{5}$$

Due to the assumptions, right after the impact the center-of-mass velocity changed only in direction whereas the angular velocity and the tangential velocity v_t remain unchanged, i.e.

$$-v_{\mathrm{cm},x}(t_0) = v_\mathrm{t}(t_0). \tag{6}$$

The rolling condition is no longer fulfilled and kinetic friction forces act on the ball.

2.2. Center-of-mass and angular acceleration

To determine the center-of-mass acceleration $\vec{a}_\mathrm{cm}$ and the angular acceleration $\vec{\alpha}$ of the ball after the first impact, we apply Newton's laws of translation and rotation:

$$\vec{F}_\mathrm{net} = m\vec{a}_\mathrm{cm} \tag{7}$$

$$\text{and} \qquad \vec{\tau}_\mathrm{net} = I\vec{\alpha}. \tag{8}$$

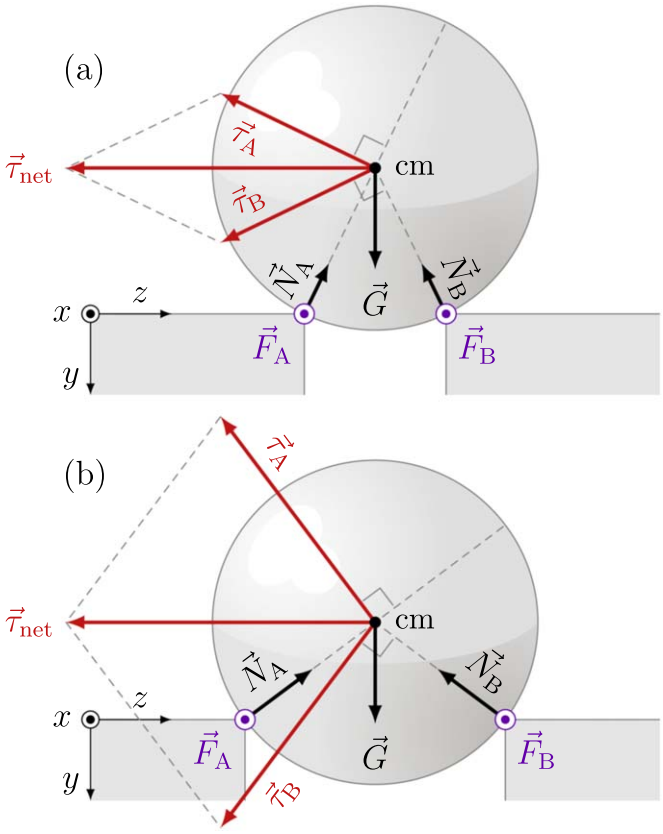

Figure 5. Torques τ_{A}, τ_{B} and τ_{net} due to the kinetic friction forces $\vec{F}_{\mathrm{A}}$ and $\vec{F}_{\mathrm{B}}$, normal forces $\vec{N}_{\mathrm{A}}$ and $\vec{N}_{\mathrm{B}}$ and weight force $\vec{G}$ for a (a) small and (b) greater groove width b. In (b) the magnitude of the kinetic friction forces is greater.

$\vec{F}_{\mathrm{net}}$ denotes the net force on the ball, $\vec{\tau}_{\mathrm{net}}$ the net torque with respect to the center of mass and $I = \frac{2}{5}mR^2$ the moment of inertia of the ball with respect to an axis passing through the center of mass.

For both laws, we need to identify all forces exerted on the ball. The groove exerts normal forces $\vec{N}_{\mathrm{A}}$ and $\vec{N}_{\mathrm{B}}$ on the ball at the contact points A and B, respectively. Because the ball moves only in or against the x-direction, the y- and z-componenst of the net force is zero. Therefore, the normal forces and the weight force in the y–z plane compensate each other, i.e.

$$\vec{N}_{\mathrm{A}} + \vec{N}_{\mathrm{B}} = -mg\vec{e}_y. \tag{9}$$

Due to symmetry, the y-components of the normal forces are

$$N_{\mathrm{A/B},y} = -\frac{1}{2}mg. \tag{10}$$

According to figure 5, we get

$$\frac{|N_{\mathrm{A/B},y}|}{|\vec{N}_{\mathrm{A/B}}|} = \frac{r}{R} = k, \tag{11}$$

with the ratio

$$k = \frac{r}{R} = \sqrt{1 - \left(\frac{b}{2R}\right)^2}, \tag{12}$$

derived from figure 4. From (10) and (11) we get

$$|\vec{N}_{\mathrm{A/B}}| = \frac{1}{2k} mg. \tag{13}$$

The normal forces produce kinetic friction forces $\vec{F}_{\mathrm{A}}$ and $\vec{F}_{\mathrm{B}}$ at the A and B contact points, respectively. These forces point in the x-direction, because they are opposed to the velocity

$$v_{\mathrm{A/B},x}(t_0) = v_{\mathrm{cm},x}(t_0) - r\omega_z(t_0) = 2v_{\mathrm{cm},x}(t_0) < 0 \tag{14}$$

in the x-direction. Application of the kinetic friction law yields

$$\vec{F}_{\mathrm{A/B}} = \mu_{\mathrm{k}} |\vec{N}_{\mathrm{A/B}}| \vec{e}_x = \frac{1}{2k} \mu_{\mathrm{k}} mg \vec{e}_x, \tag{15}$$

where μ_{k} is the coefficient of kinetic friction. Overall, the net force on the ball is

$$\vec{F}_{\mathrm{net}} = \vec{F}_{\mathrm{A}} + \vec{F}_{\mathrm{B}} + \underbrace{\vec{N}_{\mathrm{A}} + \vec{N}_{\mathrm{B}} + \vec{G}}_{=\vec{0}} = \frac{1}{k} \mu_{\mathrm{k}} mg \vec{e}_x. \tag{16}$$

According to (7) the center-of-mass's acceleration

$$\vec{a}_{\mathrm{cm}} = \frac{1}{k} \mu_{\mathrm{k}} g \vec{e}_x \tag{17}$$

is constant, independent from the balls' mass and dependent on the groove width.

For each force, we calculate the torque with respect to the center of mass. The lines of action of the normal forces $\vec{N}_{\mathrm{A/B}}$ and the weight force $\vec{G}$ pass through the center of mass, thus their torques are zero. The kinetic friction force $\vec{F}_{\mathrm{A}}$ and $\vec{F}_{\mathrm{B}}$ causes the torque $\vec{\tau}_{\mathrm{A}}$ and $\vec{\tau}_{\mathrm{B}}$, respectively. The torques are

$$\vec{\tau}_{\mathrm{A/B}} = (\vec{r}_{\mathrm{A/B}} - \vec{r}_{\mathrm{cm}}) \times \vec{F}_{\mathrm{A/B}}. \tag{18}$$

Inserting (3) and (15) in (18) yields

$$\vec{\tau}_{\mathrm{A/B}} = (r\vec{e}_y \mp \tfrac{b}{2}\vec{e}_z) \times \left(\tfrac{1}{2k}\mu_{\mathrm{k}} mg \vec{e}_x\right) = -\tfrac{1}{2k}\mu_{\mathrm{k}} mgr\vec{e}_z \mp \tfrac{b}{4k}\mu_{\mathrm{k}} mg\vec{e}_y. \tag{19}$$

Hence, the y-component of the net torque $\vec{\tau}_{\mathrm{net}} = \vec{\tau}_{\mathrm{A}} + \vec{\tau}_{\mathrm{B}}$ is zero and we get

$$\vec{\tau}_{\mathrm{net}} = -\frac{1}{k}\mu_{\mathrm{k}} mgr\vec{e}_z = (r\vec{e}_y) \times (2\vec{F}_{\mathrm{A/B}}) = -R\mu_{\mathrm{k}} mg\vec{e}_z. \tag{20}$$

The net torque τ_{net} is independent of the groove width b, because for increasing b the normal forces and the kinetic friction forces, and thus their torques, increase, but also the angle between the torques (figure 5). According to (8) and (20) the angular acceleration

$$\vec{\alpha} = -\frac{5\mu_{\mathrm{k}} g}{2R}\vec{e}_z \tag{21}$$

is constant and independent from the balls' mass and the groove width.

2.3. Interplay between translation and rotation

Integrating (17) and (21) over the time intervall $[t_0, t]$ yields, with (6), the linear functions

$$v_{\mathrm{cm},x}(t) = v_{\mathrm{cm},x}(t_0) + \frac{\mu_\mathrm{k} g}{k} t, \tag{22}$$

$$v_\mathrm{t}(t) = \omega_z(t) r = -v_{\mathrm{cm},x}(t_0) - \frac{5k\mu_\mathrm{k} g}{2} t. \tag{23}$$

The signs in (22) and (23) indicate that the graphs of $v_{\mathrm{cm},x}(t)$ and $v_\mathrm{t}(t)$ have for all k an intersection point at time t_0' (figure 6), when the ball fulfills the rolling condition after the first impact, i.e.

$$v_{\mathrm{cm},x}(t_0') = v_\mathrm{t}(t_0'). \tag{24}$$

From (22)–(24) we obtain for t_0', $v_{\mathrm{cm},x}(t_0')$ and the position $x(t_0') = \int_0^{t_0'} v_{\mathrm{cm},x}(t)\,\mathrm{d}t$:

$$t_0' = -\frac{4k}{2 + 5k^2} \frac{v_{\mathrm{cm},x}(t_0)}{\mu_\mathrm{k} g} > 0 \tag{25}$$

$$v_{\mathrm{cm},x}(t_0') = -\frac{2 - 5k^2}{2 + 5k^2} v_{\mathrm{cm},x}(t_0) = v_\mathrm{t}(t_0') \tag{26}$$

$$x_\mathrm{cm}(t_0') = -\frac{20k^3}{2 + 5k^2} \frac{v_{\mathrm{cm},x}^2(t_0)}{\mu_\mathrm{k} g} < 0. \tag{27}$$

Equation (26) allows one to discriminate between the three trajectory types:

- $v_{\mathrm{cm},x}(t_0') < 0$ for $b \in (0, b^*)$: the ball performs pure rolling for $t > t_0'$ against the x-direction and the balls move apart from each other. The center-of-mass velocity $v_{\mathrm{cm},x}$ remains negative after the impact, but the tangential velocity v_t and the angular velocity $\vec{\omega}$ change their direction according to (23) at a time

$$t_0^\mathrm{r} = -\frac{2}{5k\mu_\mathrm{k} g} v_{\mathrm{cm},x}(t_0) \in [t_0, t_0']. \tag{28}$$

  At this time, the ball performs pure translation (figure 3(b)).
- $v_{\mathrm{cm},x}(t_0') = 0$ for $b = b^*$, i.e. the balls come to rest at time t_0'. From (26) and (12) we get for the critical groove width

$$\frac{b^*}{R} = \sqrt{\frac{12}{5}}. \tag{29}$$

  Neither the direction of translation nor the direction of rotation change, because the rolling condition is fulfilled at the moment the center-of-mass velocity is zero.
- $v_{\mathrm{cm},x}(t_0') > 0$ for $b \in (b^*, 2R)$: the ball is rolling in the x-direction for $t \geqslant t_0'$ and the balls collide again. The direction of rotation remains the same, whereas the direction of translation changes according to (22) at a time

$$t_0^\mathrm{t} = -\frac{k}{\mu_\mathrm{k} g} v_{\mathrm{cm},x}(t_0) \in [t_0, t_0']. \tag{30}$$

  At this time the ball performs pure rotation (figure 3(a)).

Overall, the slopes of the $v_{\mathrm{cm},x}$- and the v_t-graph determine which of the three trajectory types occur. Therefore, the ratio

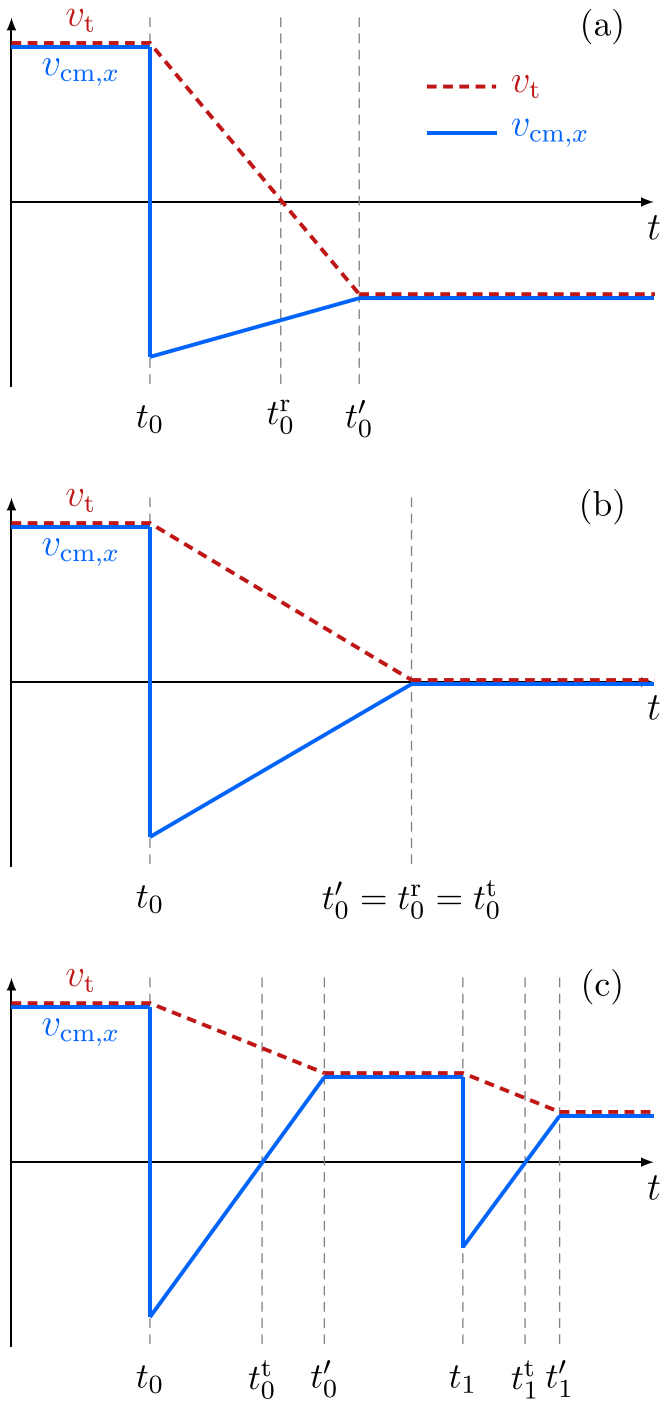

Figure 6. Theoretical graphs of the center-of-mass' velocity $v_{\mathrm{cm},x}(t)$ and the tangential velocity $v_\mathrm{t}(t)$ for groove widths (a) $b \in (0, b^*)$, (b) $b = b^*$ and (c) $b \in (b^*, 2R)$.

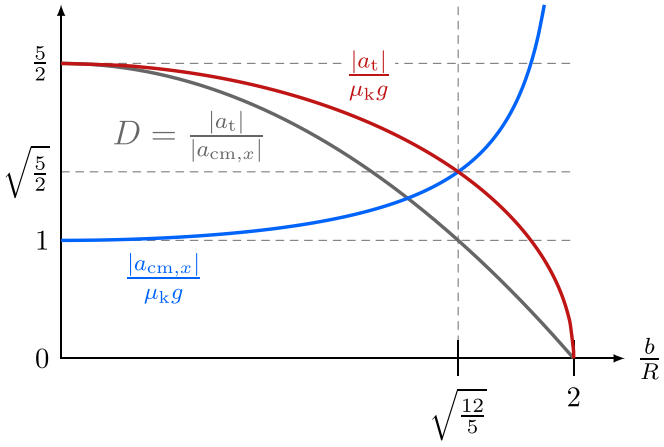

Figure 7. Normalized center-of-mass acceleration $|a_{\mathrm{cm},x}|/(\mu_\mathrm{k} g)$, normalized tangential acceleration $|a_\mathrm{t}|/(\mu_\mathrm{k} g)$ and ratio D against the ratio b/R.

$$D = \frac{|a_\mathrm{t}|}{|a_{\mathrm{cm},x}|} = \frac{5}{2}k^2 = \frac{5}{2}\left(1 - \frac{b^2}{4R^2}\right) \tag{31}$$

is a determinant for the three trajectory types, where

$$a_\mathrm{t} = \frac{\mathrm{d}v_\mathrm{t}}{\mathrm{d}}t = r\alpha_z \tag{32}$$

denotes the tangential acceleration.

For $D \in \left(1, \frac{5}{2}\right)$ and $b \in (0, b^*)$, the tangential acceleration a_t is greater than the center-of-mass acceleration $a_{\mathrm{cm},x}$ (figure 7). Translatory motion decelerates faster than rotatory motion and, therefore, the direction of translation changes before the direction of rotation can change and the balls move apart. For $D \in (0, 1)$ and $b \in (b^*, 2R)$ the roles of translation and rotation are reversed: the balls move towards each other and collide several times. For $D = 1$ and $b = b^*$ the center of mass and the tangential acceleration are equal in magnitude, i.e. the translatory and rotatory motion synchronously decelerate till the balls are at rest.

3. Comparison of theory and experiment

For groove widths b of the three corresponding trajectory types, the balls' (radius $R = 2.75$ cm, mass $m = 0.167$ kg) translatory and rotatory motion were measured with video analysis [8] by tracking the center-of-mass coordinates and the coordinates of a point on a circle of effective radius r with respect to a fixed coordinate system (frame rate of 100/s). Coordinate measurement errors were minimized by sufficiently high ball radius and a selection of smallest possible image sections, which were adapted to the ball's motion. We checked the equality of the initial ball speeds and calculated the left ball's center-of-mass velocity $v_{\mathrm{cm},x}$ and according to (4) the tangential velocity v_t (figure 8).

In order to determine the critical groove width b^* for the measurement of case (b) in figure 8, we have reduced the groove width over several tests until, at a width of $b = 4.4$ cm, the balls came to rest after the first impact. The critical case was observed for groove widths in a range of 4.1 cm to 4.4 cm, where $b^* = 4.26$ cm is the calculated critical groove width from (29).

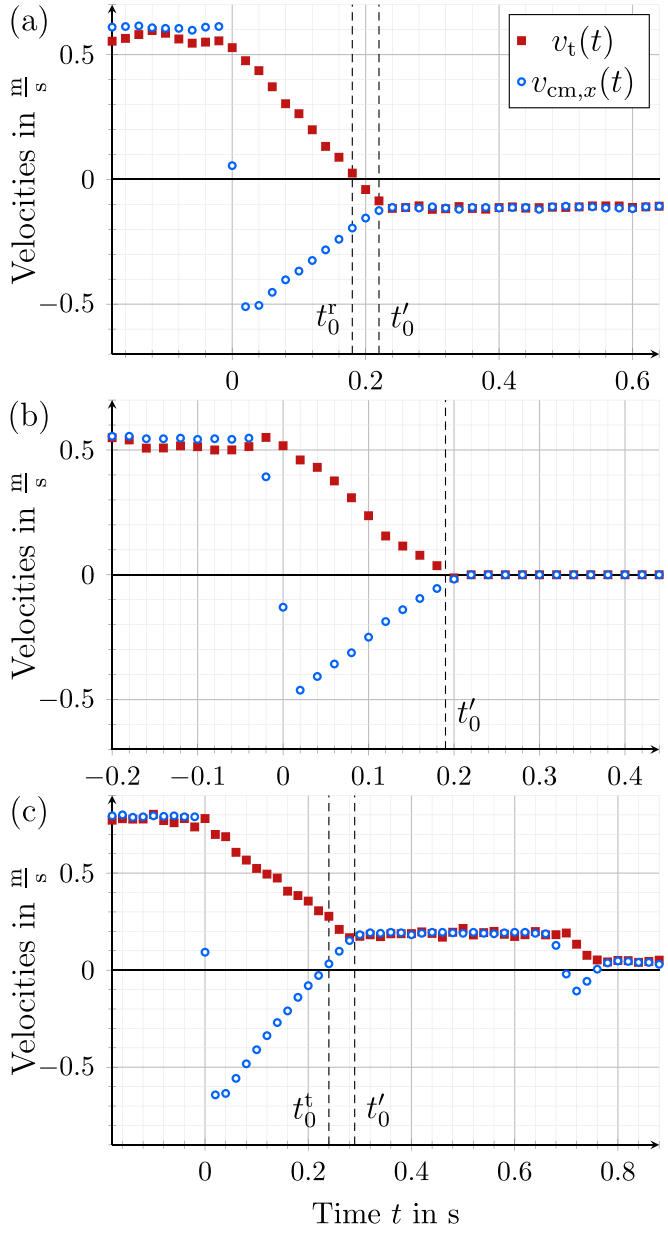

Figure 8. Measured center-of-mass velocity $v_{\mathrm{cm},x}(t)$ and tangential velocity $v_\mathrm{t}(t)$ for groove widths (a) $b = 3.5$ cm, (b) $b = 4.4$ cm and (c) $b = 4.9$ cm.

Equal magnitudes of $v_{\mathrm{cm},x}$ right before and after the collision as well as the constant $v_{\mathrm{cm},x}$ in pure rolling time intervals confirm the previously made assumptions (section 2.2). The approximately linear graphs of the intermediate motion states confirm the use of the velocity-independent kinetic friction law (15).

The center-of-mass acceleration $|a_{\mathrm{cm},x}|$ and the tangential acceleration $|a_\mathrm{t}|$ in table 1 is determined from linear regression of $v_{\mathrm{cm},x}(t)$ and $v_\mathrm{t}(t)$ in figure 8 restricted to the linear piece

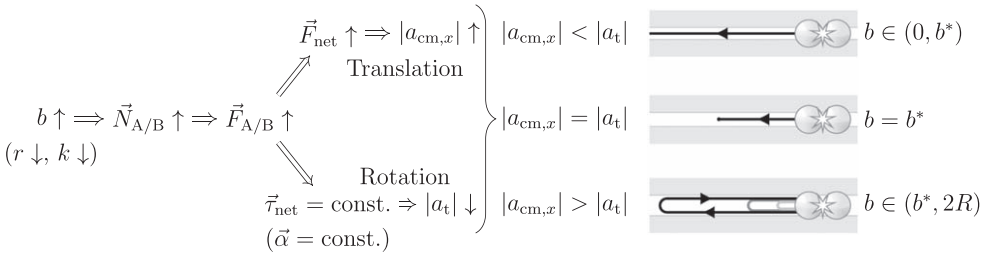

Figure 9. Cause-and-effect chain to explain the occurence of the three trajectory types with groove width b, effective radius r, ratio $k = r/R$, normal forces $\vec{N}_{\mathrm{A/B}}$, kinetic friction forces $\vec{F}_{\mathrm{A/B}}$, net force $\vec{F}_{\mathrm{net}}$, net torque $\vec{\tau}_{\mathrm{net}}$, angular acceleration $\vec{\alpha}$, center-of-mass acceleration $a_{\mathrm{cm},x}$ and tangential acceleration a_{t}. $\uparrow$ and $\downarrow$ denote increase and decrease in magnitude, respectively.

Table 1. Experimentally determined quantities for the intermediate motion states after the first collision (figure 1).

b in cm	$\lvert a_{\mathrm{cm},x}\rvert$ in m s^{-2}	$\mu_{\mathrm{k,cm}}$	$\lvert\vec{F}_{\mathrm{net}}\rvert$ in N
3.5	2.15	0.17	0.36
4.4	2.86	0.18	0.48
4.9	3.26	0.17	0.54
b in cm	$\lvert a_{\mathrm{t}}\rvert$ in m s^{-2}	$\mu_{\mathrm{k,t}}$	$\lvert\vec{\tau}_{\mathrm{net}}\rvert$ in Nm
3.5	2.92	0.15	0.008
4.4	2.61	0.17	0.009
4.9	2.00	0.16	0.008

after the first collision. From both accelerations the kinetic friction coefficient $\mu_{\mathrm{k,cm}}$ and $\mu_{\mathrm{k,t}}$ is calculated from the slope formula in (22) and (23), respectively. We used $\mu_{\mathrm{k}} = \mu_{\mathrm{k,cm}}$ in (16) and (20) to calculate the net force $|\vec{F}_{\mathrm{net}}|$ and the net torque $|\vec{\tau}_{\mathrm{net}}|$ in table 1 because the center-of-mass velocity v_{cm} could be measured more accurately than the tangential velocity v_{t}. Furthermore, the times t_0', t_0^{r} and t_0^{t} in figure 8 were calculated by (25), (28) and (25) with $\mu_{\mathrm{k}} = \mu_{\mathrm{k,cm}}$ and correspond well with the measurement data.

The experimental results in table 1 indicate that in accordance with the theory (figure 7, (16) and (20)) for increasing groove width b the center-of-mass acceleration $a_{\mathrm{cm},x}$ and the net force $\vec{F}_{\mathrm{net}}$ increase and the tangential acceleration a_{t} decreases, whereas the torque $\vec{\tau}_{\mathrm{net}}$ is approximately constant. The mean kinetic friction coefficient from table 1 is $\mu_{\mathrm{k}} = 0.17$.

4. Summary and educational conclusions

In this article, we derived a cause-and-effect chain from particle kinematics and the application of Newton's laws of translation and rotation for rigid bodies to explain the three trajectory types when two identical balls collide centrally and ideal-elastically with equal speed in a groove of variable groove width (figure 9). Overall, an increasing groove width causes an increasing center of mass and a decreasing tangential acceleration in magnitude, so that when the rolling condition is fulfilled, the center-of-mass velocity either points away

from the location of collision (the balls depart), is zero (the balls come to rest) or points towards the location of collision (the balls collide again). For the chosen collision conditions the motion of the balls is symmetrical to the location of the collision and the three trajectory types arise independently of the equal initial speed of the balls.

The theoretical level of the experiment provides a challenging problem for introductory mechanics courses. Explaining the occurence of the three trajectory types in the experiment requires one to make appropriate assumptions, to apply and combine several rigid body concepts and to perform a quantitative analysis of the relations between quantities. Therefore, students should have sufficient previous knowledge about the laws and kinematics of rigid bodies from lectures. We recommend to implement the experiment with the here-presented theoretical treatment in homework problems or in an introductory physics laboratory [6], because there will be sufficient time for students to understand the experimental results on their own. Additionally, teachers can deal with the well-known difficulties students have in understanding relevant rigid body concepts concerning the experiment, for example:

- particle velocities of a rolling body with respect to a fixed and a moving coordinate system [9];
- independence of Newton's law of translation from the working point of forces [10];
- a single force on a rigid body can cause translation and rotation [10]; and
- connection of kinetic friction forces and kinematics during the transition from pure rolling to pure translation [11].

ORCID iDs

S Gröber https://orcid.org/0000-0001-7570-1889

References

[1] Doménech A and Casasús E 1991 *Phys. Educ.* **26** 186–9
[2] Redner S 2004 *Am. J. Phys.* **72** 1492–8
[3] Hierrezuello J 1993 *Phys. Educ.* **30** 177–82
[4] Hopkins D C and Patterson J D 1977 *Am. J. Phys.* **45** 263–6
[5] Wallace R E and Schroeder M C 1988 *Am. J. Phys.* **56** 815–9
[6] Hanisch C, Hofmann F and Ziese M 2018 *Eur. J. Phys.* **39** 015003
[7] Serway R and Jewett J 2012 *Physics for Scientists and Engineers, Chapters 1-39* (*Available 2010 Titles Enhanced Web Assign Series*) (Boston, MA: Cengage Learning)
[8] Allain R 2016 *Physics and Video Analysis* (San Rafael, CA: Morgan & Claypool Publishers)
[9] Rimoldini L G and Singh C 2005 *Phys. Rev. Phys. Educ. Res.* **1** 010102
[10] Close H G, Gomez L S and Heron P R L 2013 *Am. J. Phys.* **81** 458–70
[11] Ambrosis A, Malgieri M, Mascheretti P and Onorato P 2015 *Eur. J. Phys.* **36** 035020